



Design of vertical rockfill breakwaters

Paul MILESI¹, Olivier KIMMOUN², David LAJOIE¹

1. SAS Hydro GC, 772 chemin du Flaquier Nord 06530 Le Tignet, France.

paul.milesi@hydrogc.fr

2. Ecole Centrale Marseille, 38 rue Frédéric Joliot-Curie 13013 Marseille, France.

olivier.kimmoun@centrale-marseille.fr

Abstract:

Vertical riprap structures are innovative and alternative systems to vertical caissons. The blocks are enclosed by a metal framework or drilled piles occupying a reduced ground footprint. This type of structure offers many advantages: low impact during construction, possibility of implanting near areas of marine life without significant impact, permeability for currents. As part of the redevelopment of the port of Banyuls-sur-Mer, the construction of a 20 m diameter verticalized rockfill breakwater significantly improves the quality of the harbor basin and respect the surrounding seagrass. An easy-use numerical model of 2D/3D diffraction with integral equations has been developed to test different configurations of structures, combining for example Jarlan caissons and rocks. Physical scale models have confirmed the functioning of simple porous structures.

Paper selected during the colloquium

"XVèmes Journées Nationales Génie Côtier Génie Civil", La Rochelle (France), 29-31 May 2018.

Received 13 June 2019, accepted 23 October 2021, available online 22 November 2021.

Short translated version not certified, published under the responsibility of the authors.

How to cite the original paper:

MILESI P., KIMMOUN O., LAJOIE D. (2021). *Conception d'ouvrages côtiers verticaux en enrochements*.
Revue Paralia, Vol. 14, pp s01.1–s01.12.

DOI: <https://doi.org/10.5150/revue-paralia.2021.s01>

1. Introduction

Design studies for new maritime structures in the French coastal zone are generally carried out as part of the development of existing ports. The extension of basin surfaces and the improvement of agitation are the main axes of development of marinas, often justifying investments in terms of infrastructure. This is for example the case of the redevelopment of the marina of Banyuls-sur-Mer (66), which is an opportunity to significantly improve the quality of its port basin by, among other things, the lengthening of the main dike.

The extension of coastal structures has for many years involved the respect of the environment. The very wide rubble-mound breakwaters, built at the beginning of the 20th century to delimit the deep-water port basins, have been gradually replaced by vertical caisson-type structures that are more economical and consume less quarry materials. The footprint on the seabed is reduced. Other alternatives to vertical concrete damping breakwaters have been designed, such as vertical rockfill structures. The blocks are held by a metal structure or piles. This type of structure offers the possibility of being located near areas of marine life without significant impact.

In Banyuls-sur-Mer, the construction of a 20 m diameter vertical rockfill breakwater in a metal frame may curb the problems of port agitation today encountered with the swells of storms from the South-East (Figure 1). The protected seagrass areas are by this process kept at least 5m from the foot of the structure.

Research work has been undertaken to model the interaction between waves and vertical porous rockfill structures.

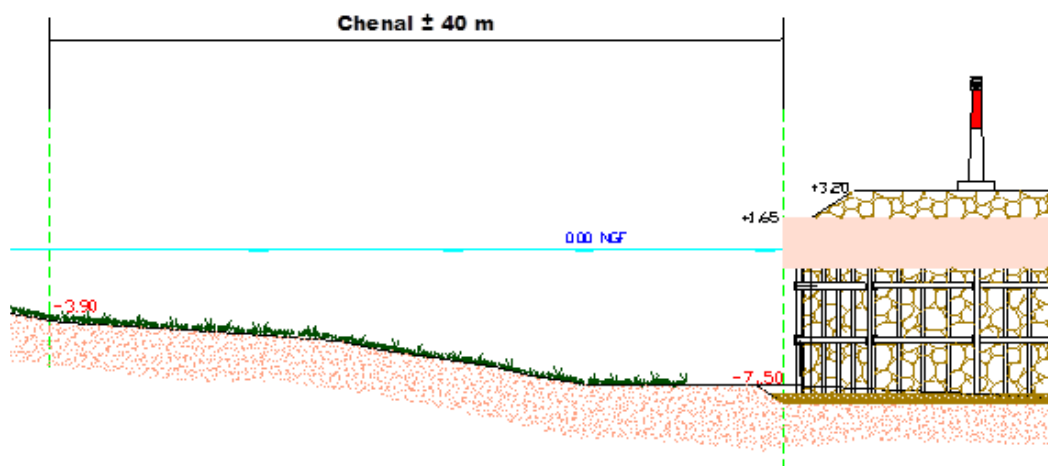


Figure 1. Configuration of the vertical breakwater.

2. Experimental setting

The tests were carried out in the 17 m length by 60 cm wide wave flume of the Ecole Centrale de Marseille and fitted with a wave-making machine. A damper pad is set at the end of the flume. Froude's similarity to the 1/10th scale reproduces the forces applied to the fluid whose flow is turbulent in the porous medium. The model is a cage with a steel structure to contain the blocks that will dissipate the energy of the incident swell. The model is 24 cm wide. The water height is 20 cm.

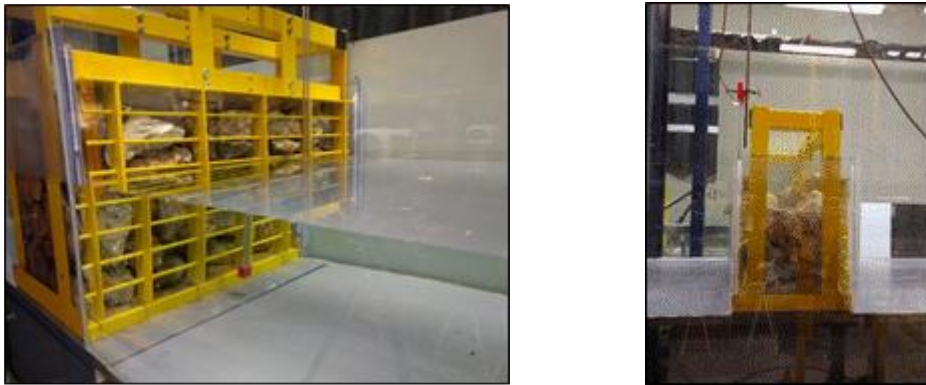


Figure 2. Oblique and lateral views of the model.

Limestones are used for the campaign whose average density of a typical sample was measured at $\rho \approx 2620 \text{ kg.m}^{-3}$. First, three typical grain sizes were selected to investigate the influence of rock size and porosity rate on the hydrodynamic characteristics of the structure. The rocks were weighed one by one before each series of tests in order to determine the particle size curve corresponding to the sample in place as well as to determine the porosity. The typical grain sizes used in the campaign are as follows:

The net change in the median mass M_{50} between the standard particle sizes induces a very slight change in the corresponding porosity rate. The spread of the porosity rates is quite limited with $41.5\% \leq n \leq 44.8\%$. They are in the upper range of realistic porosity rates defined by VAN GENT (1995), $35\% \leq n \leq 45\%$. The presence of the walls of the cage compared to a "free" stacking of the rocks could explain these high porosities as proposed by MELLINK (2012). The arrangement of the rocks also had an impact, at most 2%, on the calculated porosity rates.

Table 1. Characteristics of particle size curve.

Type of particle size curve	M_{10}	M_{50}	M_{85}	D_{n50}	n_{RRD}	Porosity n
G1	170 g	233 g	282 g	4.5 cm	17.2	41.5%
G2	527 g	617 g	716 g	6.2 cm	28.4	43.6%
G3	1204 g	1861 g	2647 g	8.9 cm	11.0	44.8%

3. Experimental results

The reflection and transmission coefficients in regular waves are computed using a separation method developed by ANDERSEN *et al.* (2017). Two sets of five limnometric probes were placed on either side of the model. The measurement uncertainties are mainly due to the calibration of the probes. The hydrodynamic performance of a structure in damping the incident swell can be synthesized by calculating the dissipated energy E_d :

$$E_d = 1 - (k_r^2 + k_t^2) \quad (1)$$

k_r and k_t are respectively the reflection and transmission coefficients. The energy dissipated E_d by the porous structure is significantly higher for small periods than for large ones. It logically decreases as the wavelengths increase in front of the model. The performance of the structure is also better at large amplitudes. This is explained by the presence of higher speeds and by greater dissipation due to the turbulent friction term in v^2 . The curves below (Figure 3) present the results of the hydrodynamic performance for the incident wave height $a_i=2.5$ m.

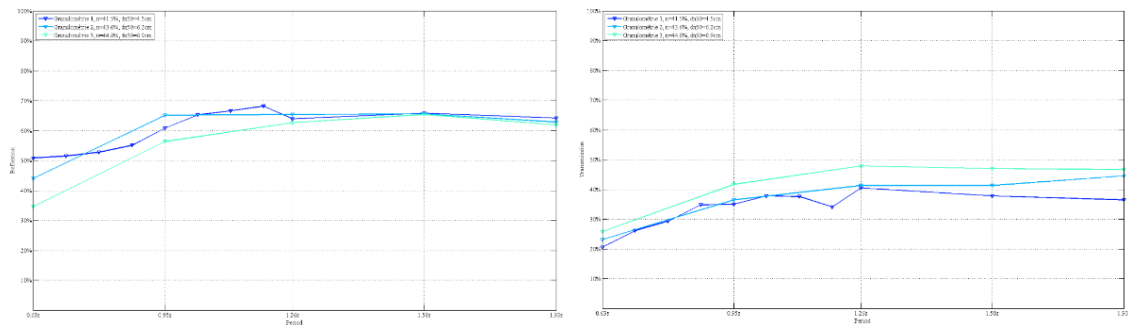


Figure 3. Comparison of particle size curves 1, 2 and 3, $a_i=1.25$ cm

4. Flow modelling generated by swell in porous medium

A closed volume containing the porous medium is defined. The conservation of the momentum within the domain is expressed as:

$$\iiint_F \left(\frac{\partial \vec{v}}{\partial t} + \vec{v} \cdot \overrightarrow{\text{grad}} \vec{v} \right) dV = -\frac{1}{\rho} \iint_{\partial \Sigma} p d\vec{S} + \iiint_{\Sigma} \vec{f}_r dV + \iiint_F \vec{g} dV \quad (2)$$

with: \vec{f}_r are the friction forces on the microscopic scale, Σ is the global domain, F the fluid domain, $\partial \Sigma$ the exterior surface of the domain Σ , and \vec{v} the infiltration speed. At the macroscopic scale, for a non-stationary flow in a porous medium, the friction forces can be modelled by the FORCHHEIMER (1901) equation extended by POLUBARINOVA-KOCHINA (1952) who added an inertia term:

$$\vec{F}_r = - \left[a \vec{v}_d + b \|\vec{v}_d\| \vec{v}_d + c \frac{\partial \vec{v}_d}{\partial t} \right] \quad (3)$$

a, b and c are coefficients specific to the considered porous medium, \vec{v}_d is the flow velocity (Darcy) defined by $\vec{v}_d = n \vec{v}$, where n is the porosity rate.

The friction coefficients used are those of BURCHARTH and ANDERSEN (1995), other coefficients giving an underestimation of the transmission:

$$a = \alpha \frac{(1-n)^2}{n^3} \frac{v}{d_{n50}^2} \quad b = \beta \frac{1-n}{n^3} \frac{1}{d_{50}} \quad c = \frac{(1-n)}{n^2} C_m \quad (4)$$

with: d_{n50} is the nominal median diameter of the blocks, α and β are coefficients of tortuosity, C_m is a coefficient of added mass. Equation (2) can be rewritten on a macroscopic scale by introducing the flow velocity \vec{v}_d :

$$S \frac{\partial \vec{v}_d}{\partial t} + \frac{1}{2n^2} \overrightarrow{\text{grad}} \vec{v}_d^2 = -\frac{1}{\rho} \overrightarrow{\text{grad}} p - g\vec{z} - \frac{v}{K} \vec{v}_d - \frac{C_f}{\sqrt{K}} \|\vec{v}_d\| \vec{v}_d \quad (5)$$

where the relations between the coefficients (a, b, c) and the friction coefficients (K, C_f) and inertia S (SOLLIT & CROSS, 1972) are:

$$K = \frac{v}{a} \quad C_f = b\sqrt{K} \quad S = \frac{1}{n} + c \quad (6)$$

Equation (5) is linearized using the LORENTZ procedure. The dissipation term is replaced by a linear expression, by introducing a dimensionless dissipation coefficient $f\omega$ such as:

$$f\omega = \frac{v}{K} + \frac{C_f}{\sqrt{K}} \overline{v}_d \quad (7)$$

with:

$$\overline{v}_d = \frac{\iiint_P \int_0^T |\vec{v}_d|^3 dt}{\int_0^T |\vec{v}_d|^2 dt} \quad (8)$$

The flow in the continuous fluid medium external to the porous medium is assumed to be irrotational, hence the existence of a potential of velocities Φ_F . The porous medium is considered as a continuous medium and a potential of velocities is also introduced into it Φ_p .

By neglecting the quadratic term in $\overrightarrow{\text{grad}} \vec{v}_d^2$ and replacing \vec{v}_d with $\overrightarrow{\text{grad}} \Phi_p$, it results:

$$S \frac{\partial \Phi_p}{\partial t} + \frac{p_p}{\rho} + gz + f\omega \Phi_p = 0 \quad (9)$$

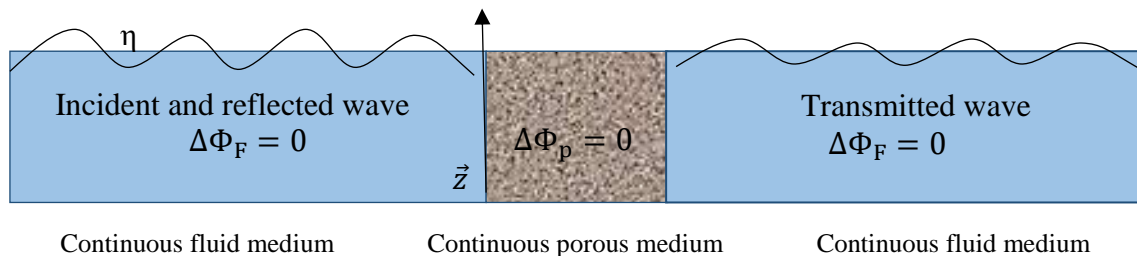


Figure 4. Theoretical and experimental configuration.

5. Numerical results

The harmonic system is solved by a singularity method based on a mixed distribution of RANKINE sources and doublets. Continuity of flows and pressures is ensured at the fluid or porous media interfaces. The nonlinearity in the term $f(\vec{v}_d)$ is calculated by successive iterations until convergence.

The results of the tests and the corresponding simulations for a wave height $a_i = 25$ cm at the real scale are reported below (Figure 5, see particle size curves 1, 2 and 3). The relative root mean square error (RMSE) is given for guidance. The results of the numerical model with respect to the experimental data are satisfactory with however an underestimation of the transmission for the small rocks.

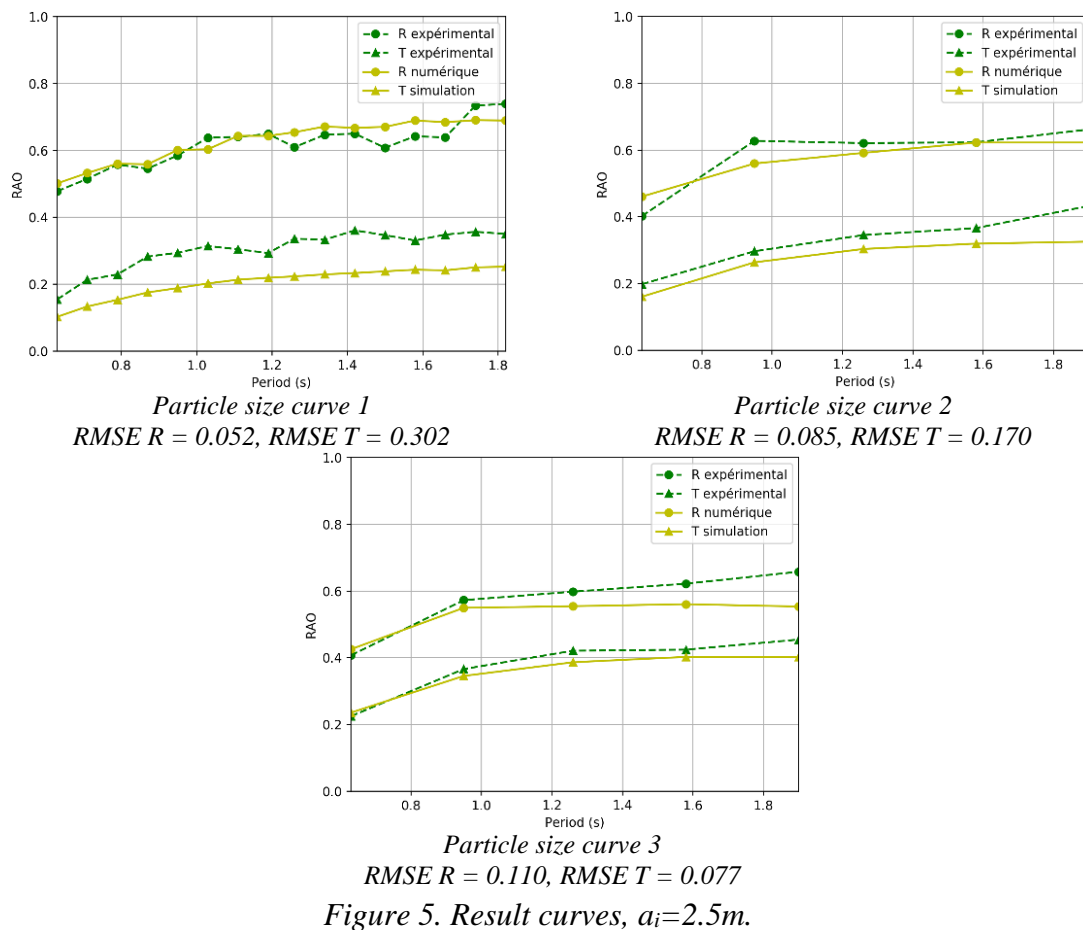


Figure 5. Result curves, $a_i=2.5m$.

6. Application: riprapp and Jarlan caisson

The numerical tool makes it possible to compute the effectiveness of structures of original design, for example, assemblies of vertical rockfill structures, more or less spaced, so as to create new pressure drops that would be added to those already present in a simple porous medium, or by coupling rocks and conventional porous walls of Jarlan type. The installation of rocks inside a Jarlan caisson plays on its hydrodynamic performance while

providing ballast and areas suitable for the development of juveniles. The examples of tested configurations are shown below in Figure 6. The configurations 1 and 2 correspond to classic Jarlan boxes with respective chamber lengths of 3.70 m and 1.85 m. In configurations 3 and 4, a porous medium is placed over 1.85 m in length and the size of the blocks is changed. The reflection coefficient in the curves below change with the period for the different configurations described. The peak performance of a Jarlan caisson is when $0.10 < B/\lambda < 0.15$.

The rocks setting inside the chamber modulates the performance of the Jarlan chamber. The optimal period of dissipation moves between the two periods associated with the length of the chamber without rocks.

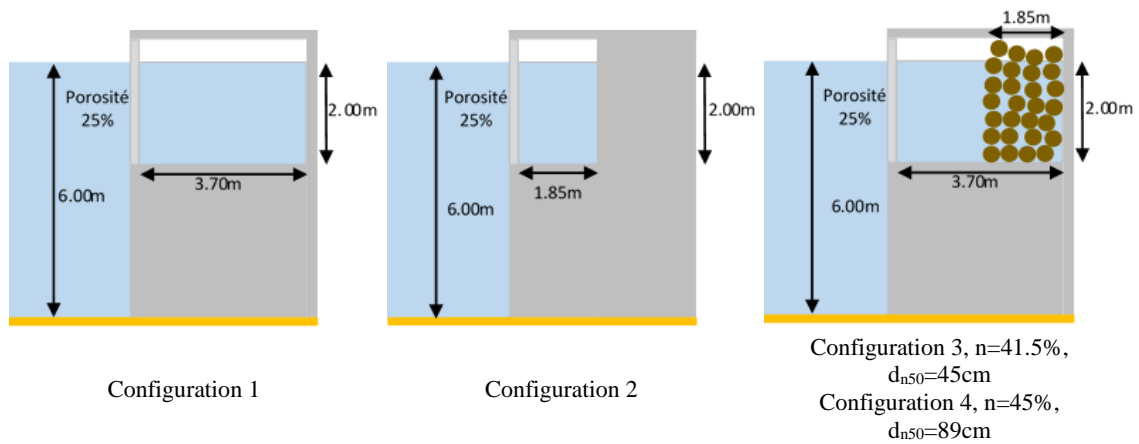


Figure 6. Sketches of tested configurations.



Figure 7. Efficiency of different configurations.

7. Conclusion

The verticalized rockfill damping structures are innovative design structures that respect the seagrass beds by limiting the impact on the ground while providing additional protection to the port basins, as is the case for the port of Banyuls-sur-Mer. They can easily be combined with other more classic breakwaters such as Jarlan caissons. The numerical tool developed should make it possible to identify the best possible

compositions between riprap and conventional structures to improve original designs combining technical and environmental constraints.

8. References

- ANDERSEN T.L., ELDRUP M.R., FRIGAARD P. (2017). *Estimation of incident and reflected components in highly nonlinear regular waves*. Coastal Engineering, Vol. 119, pp 51-54. <https://doi.org/10.1016/j.coastaleng.2016.08.013>
- BURCHARTH H.F., ANDERSEN O.H. (1995). *On the one-dimensional steady and unsteady porous flow equation*. Coastal Engineering, Vol. 24, pp 233-257. [https://doi.org/10.1016/0378-3839\(94\)00025-S](https://doi.org/10.1016/0378-3839(94)00025-S)
- FORCHHEIMER P. (1901). Wasserbewegung durch Boden, Z. Ver. Deutsch. Ing. 45, 1782–1788.
- MELLINK B. (2012). *Numerical and experimental research of wave interaction with a porous breakwater*. Thesis, Delft University of Technology.
- LAJOIE D. (2008). *Optimisation du fonctionnement des atténuateurs de houle de type "dos de chameau" à l'aide de perforations dans la structure*. X^{èmes} JNGCGC, Sophia Antipolis, pp 749-760. <http://dx.doi.org/10.5150/jngcgc.2008.071-L>
- POLUBARINOVA-KOCHINA P.Y. (1952). *Theory of ground water movement*. Gostekhizdat Moscow (in russian), English transl. by R.J.M. DE WIEST, (1962), Princeton University Press.
- SOLLIT C.K., CROSS R.H. (1972). *Wave transmission through permeable breakwaters*, 13th Coast. Eng. Conf., Vol. 3, ASCE, Vancouver, pp 1827-1846. <https://doi.org/10.9753/icce.v13.99>
- VAN GENT M.R.A. (1995). *Wave interaction with permeable coastal structures*. Thesis, Delft University of Technology.